Impact of ice-phase microphysics on inner-core processes in simulated extremely intense tropical cyclones

Sachie Kanada
HyARC, Nagoya University
Akiyoshi Wada
Meteorological Research Institute/Japan Metrological Agency
Kazuhisa Tsuboki
HyARC, Nagoya University

1. Introduction

Best track data have reported that most extremely intense tropical cyclones (TCs) such as Categories 4 and 5 based on the Saffir-Simpson Hurricane Scale (http://www.nhc.noaa.gov/aboutsshws.php) underwent rapid intensification (RI) (Kaplan and DeMaria, 2003). RI is often accompanied by secondary eyewall formation (SEF) and eyewall replacement cycles (ERC), which are closely related to the inner-core processes. However, the physical mechanisms associated with RI, SEF and ERC and relevant inner-core processes have not been fully understood. The purpose of this study is to examine the impacts of ice-phase microphysics and boundary layer processes on the inner-core processes of an extremely intense TC with RI by using two types of 2-km mesh non-hydrostatic models (NHM2).

2. Model and experimental design

We conducted sensitivity numerical experiments by using two kinds of NHM2, a non hydrostatic model based on the Japan Metrological Agency operational mesoscale model (hereafter, JMANHM: Saito et al. 2007) and the Cloud Resolving Storm Simulator (hereafter, CReSS: Tsuboki and Sakakibara 2002) developed in HyARC, Nagoya University, respectively (Table 1). Initial and boundary conditions were provided from 6-hourly results of future-climate numerical experiments performed by a 20-km mesh atmospheric general circulation model (AGCM20). A case of an extremely intense TC with the minimum central pressure (hereafter, MCP) in the results of AGCM20 was selected. Note that, the effect of a cold wake on tropical cyclone intensity is not considered since both the AGCM20 and JMANHM are not an ocean-coupling model. This assumption is valid in a region where the isotherm of 26˚C is deep enough to neglect the effect of a cold wake induced by tropical cyclones in the present-day climate (Wada and Chan, 2008).

Experimental configurations in NHM2 included 1-moment and 2-moment bulk-type microphysics with an ice-phase along with a second-order turbulence closure scheme (the MYNN scheme) and a 1.5-order turbulence closure scheme (Table 2). More information on NHM2 was described in Kanada et al. (2012 and 2013).

Table 1 Model descriptions of two types of 2-km mesh non-hydrostatic models

	JMANHM	CReSS
Horizontal resolution	2km	
Equations	Non–hydrostatic and compressible	
Horizontal grid number	900～1500 ×900～1500	
Cumulus parameterization	None	
Time step	4s	4s
Initial time	1200Z23SEP2098	
Integration time	4-5 days	
Model	Atmospheric	Atmospheric-Ocean (Slab)

Table 2 List of sentivity experiments

model	name	Turbulence	cloud microphysics	vertical layer
AGCM	AGCM20	-	-	-
JMANHM	2LK	MYNN Level 3	2-moment: Prognostic variables [*qc, qr, qi, qs, qg*] and [*Ni, Ns, Ng*]	55
	2ddLK	Deardorff	2-moment	55
	2ddLK64	Deardorff	2-moment	64
CReSS	2CRS	Deardorff	1-moment: Prognostic variables [*qc, qr, qi, qs, qg*]	64
	2CRSDB	Deardorff	2-moment	64

3. Results

The results indicated that all experiments conducted by NHM2 exhibited RI, defined as a decrease in central pressures of 42 hPa during less than 24 hours (Fig. 1). Meanwhile, in the AGCM20 experiment, the maximum pressure drop for 24 hours was 38 hPa.

Even there were no large differences in the typical intensity metrics for TC (e.g. MCP and the maximum wind speed: MWS) in all experiments by NHM2 (Table 3), differences were found substantially in the inner-core structures and horizontal distributions of precipitation and wind at 10 m (Table 3 and Fig. 2). In particular, most experiments exhibited SEF and ERC processes (Fig.2). Only the exception was the experiment by CReSS with a 1-moment microphysics (2CRS). Other features found in the sensitivity experiments were that TCs calculated by CReSS had larger radii of MWS (hereafter R_mws) and maximum azimuthally averaged precipitation (hereafter R_prec) than those of TCs by JMANHM (Table 3).

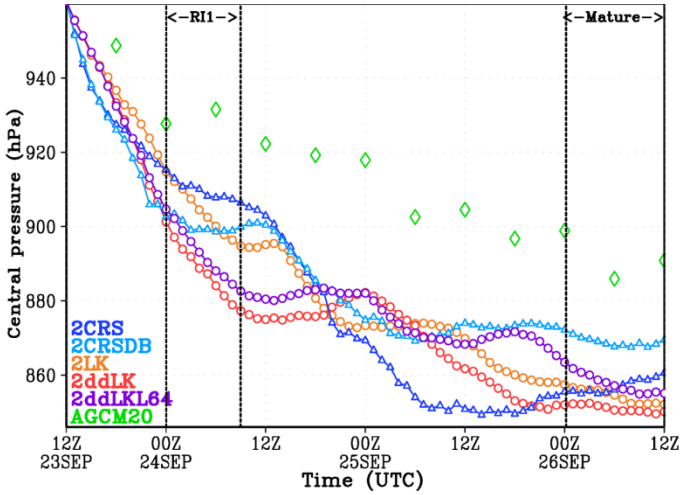

FIG. 1 Time evolution of central pressures.

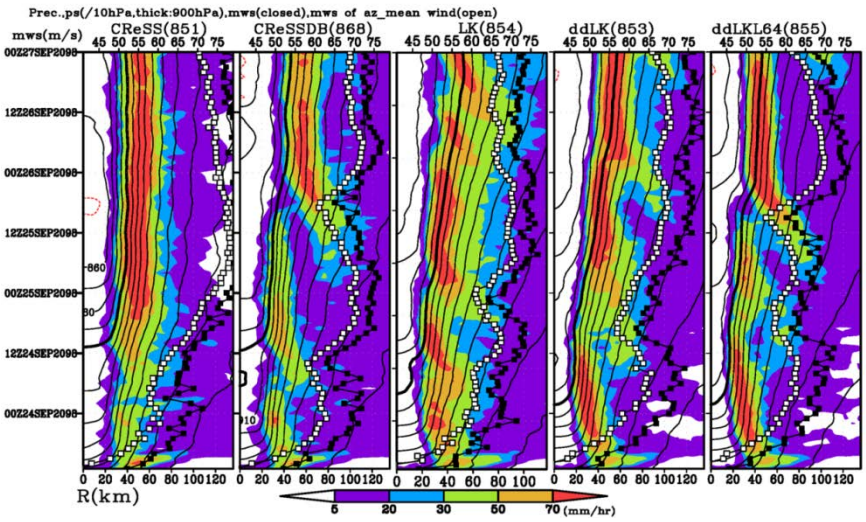

FIG. 2 Hovmoller diagram of azimuthally averaged precipitation (shaded) , maximum 10-m wind speed (closed-square) and maximum azimuthally averaged 10-m wind speed (open-square).

Table 3 Maximum central pressure (MCP: hPa), maximum wind speed (MWS: m s^{-1}), radius of MWS (R_mws: km) and radius of maximum azimuthally averaged precipitation (R_prec: km) at the time when the MCPs were marked in each experiment.

	MCP	MWS	R_mws	R_prec
AGCM20	863	79	62	62
2LK	854	77	32	36
2ddLK	853	79	36	40
2ddLK64	855	75	30	34
2CRS	851	82	32	50
2CRSDB	868	77	52	66

During the RI1 phase shown in Fig. 1, the central pressure drops exceeded 2.5 hPa $1h^{-1}$ for more than 12 hours (hereafter, E-RI) in the experiments by JMANHM with a 1.5-order turbulence closure scheme (2ddLK and 2ddLK64, see Table 2), while TCs in the CReSS experiments (2CRS and 2CRSDB, see Table 2) tended to undergo slower development. The horizontal distributions of precipitation showed that TCs with E-RI (2ddLK and 2ddLK64) had a distinct smaller, round and axisymmetric eye during the RI1 phase (Fig. 3). Mean azimuthally averaged radial-vertical cross sections of the inner-core (Fig. 4) indicated that more intense and taller updrafts at the eyewall were formed for the TCs with E-RI. Also, those TCs with E-RI had shallow inflow boundary layer accompanied by intense near-surface inflows. According to Kanada et al. (2012), the experiments by a 1.5-order turbulence closure scheme tended to form shallow inflow boundary layer with intense near-surface inflows compared to those by a second-order turbulence closure scheme. Intense near-surface inflows led to enhance an intense and tall updraft at the eyewall during the RI1 phase.

Differences between the experiments by CReSS and JMANHM were also significant in the distributions of ice-phase water substances. In the experiments by CReSS, a great amount of graupel (hereafter, *qg*) distributed in the inner-core, while there were a little or no snow water (hereafter, *qs*). On the other hand, *qg* were located only around the intense updraft area and a great amount of *qs* were found around the inner-core of TCs in the JMANHM experiments. The major differences in between *qg* and *qs* calculated by the two models are the fall velocity; *qg* assumes the larger fall velocity than that of *qs*. The wide distribution of *qs* in the JMANHM experiments may be related to the fact that *qs* with smaller fall velocity drifted a longer distance in the inner-core.

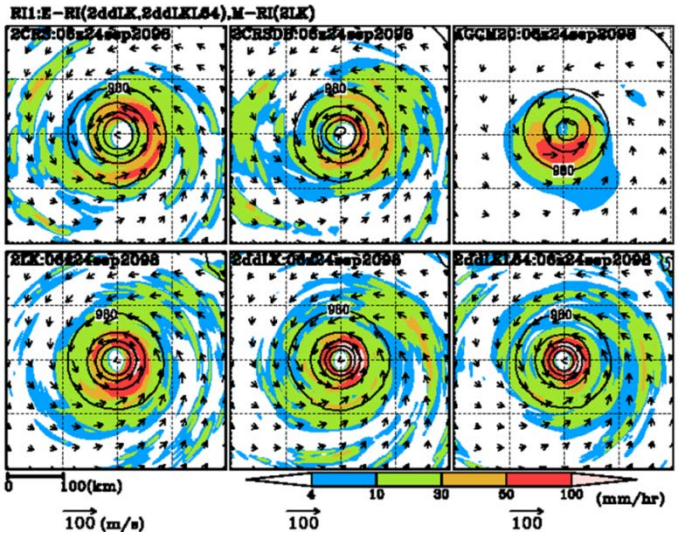

FIG. 3 Horizontal distributions of hourly precipitation amounts (shaded), sea level pressure (contour) and horizontal wind at a height of 10 m (vector) during RI1 phase (06z24sep2096) for all experiments by AGCM20 and NHM2.

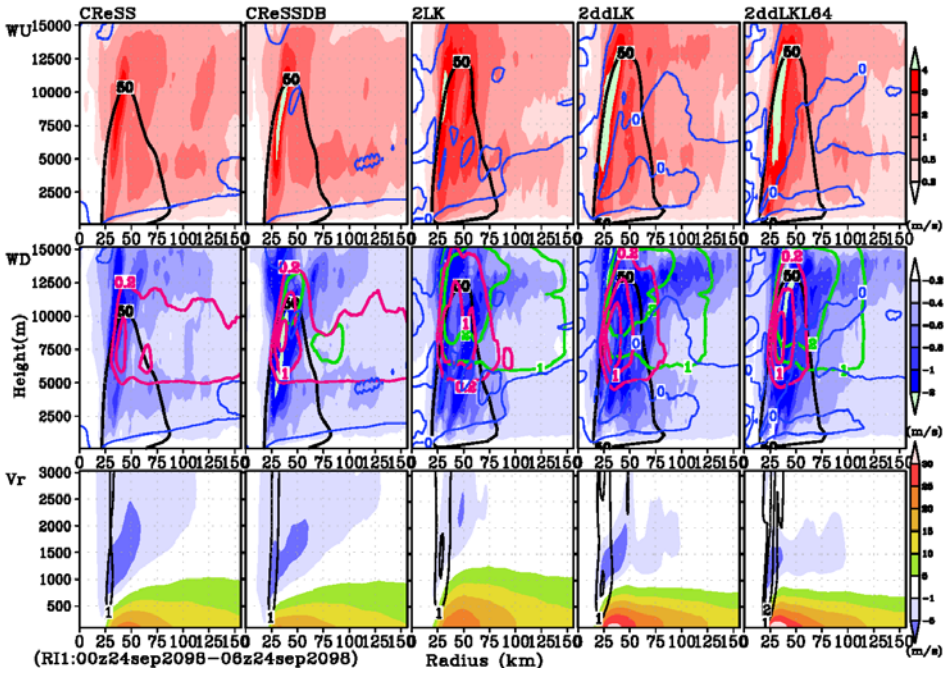

FIG. 4 Mean azimuthally averaged radial–vertical cross sections of updraft (upper), downdraft (middle) and radial wind speed below 3-km level (lower) during the RI1 phase. Black, blue, pink and green contours in the upper and middle figures denote azimuthally averaged tangential wind speeds, radial wind speeds, graupel and snow mixing ratios, respectively. Black counters in the lower figures denote vertical velocity.

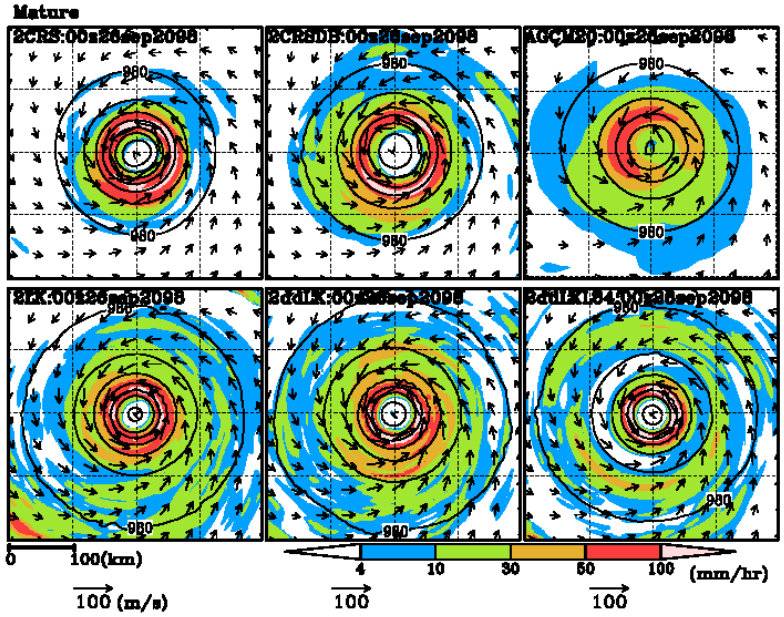

FIG. 5 Horizontal distributions of hourly precipitation amounts (shaded), sea level pressure (contour) and horizontal wind at a height of 10 m (vector) during the mature stage (00z26sep2096) for all experiments by AGCM20 and NHM2.

Finally, TCs calculated by CReSS had a larger eye with smaller horizontal expansion, while those of TCs by JMANHM had a smaller eye with larger expansion (Fig. 5).

4. Summary

To understand the impacts of ice-phase microphysics and boundary layer processes on the inner-core processes in simulated extremely intense TCs with RI, we conducted sensitivity numerical experiments using two kinds of 2-km mesh non-hydrostatic models (NHM2), JMANHM and CReSS.

All experiments conducted by NHM2 exhibited RI, defined as a decrease in central pressures of 42 hPa during less than 24 hours. In addition, shallow inflow boundary layer accompanied by intense near-surface inflows led to an intense and tall eyewall updraft during the RI phase in the experiments with E-RI. TCs calculated by CReSS had larger eyes and smaller scales of horizontal expansion with a great amount of graupel, while TCs by JMANHM had smaller eyes and larger scales of the expansion with a great amount of snow. The strength of near-surface inflows was also related to the scale of horizontal expansion. When near-surface inflow was relatively weak, the scale of horizontal expansion was small. Most experiments exhibited SEF and ERC processes. Only the exception was an experiment that snow was less calculated (CReSS with a 1-moment microphysics).

The results indicated that the ice-phase microphysics and boundary layer processes are closely related to the inner-core structures and evolutions of simulated extremely intense TCs. More important, even TCs with the similar intensity metrics, such as MCP and MWS, the characteristics of the TCs including the inner-core and horizontal expansions can be differed among non-hydrostatic models.

Acknowledgments

This study was supported by the Ministry of Education, Culture, Sports, Science and Technology of Japan under the framework of the Sousei Program. Numerical simulations were performed using the Earth Simulator.

References

Kanada, S., A. Wada and M. Sugi (2013): Future changes in structures of extremely intense tropical cyclones using a 2-km Mesh nonhydrostatic model. J. Climate, (in press)

Kanada, S., A. Wada, M. Nakano, and T. Kato, 2012: Effect of PBL schemes on the development of intense tropical cyclones using a cloud resolving model. J. Geophys. Res., 117, D03107, doi:10.1029/2011JD016582

Kaplan, J., and M. DeMaria, 2003: Large-scale characteristics of rapidly intensifying tropical cyclones in the North Atlantic basin. Wea. Forecasting, 18, 1093-1108.

Saito, K., J. Ishida, K. Aranami, T. Hara, T. Segawa, M. Narita, and Y. Honda, 2007: Nonhydrostatic atmospheric models and operational development at JMA. J. Meteor. Soc. Japan, 85B, 271-304.

Tsuboki, K., and A. Sakakibara, 2002: Large–scale parallel computing of cloud resolving storm simulator. High Performance Computing, Springer, 243–259.

Wada, A., and J. C. L. Chan, 2008: Relationship between typhoon activity and upper ocean heat content. Geophys. Res. Lett., 35, L17603, doi:10.1029/2008GL035129.